Polymer Chemistry

ROYAL SOCIETY OF CHEMISTRY

PAPER

View Article Online
View Journal | View Issue

Published on 12 July 2022. Downloaded by Institute of Chemistry, CAS on 5/7/2026 9:22:57 AM.

Check for updates

Cite this: *Polym. Chem.*, 2022, **13**, 4490

Facile synthesis of eight-membered cyclic (ester-amide)s and their organocatalytic ring-opening polymerizations†

Yu-Ting Guo, Wei Xiong, Changxia Shi, Fu-Sheng Du * and Zi-Chen Li *

Received 27th May 2022,
Accepted 11th July 2022

DOI: 10.1039/d2py00683a

rsc.li/polymers

Five eight-membered cyclic(ester-amide)s (**M1–M5**) were synthesized from phthalic anhydride and β-amino alcohols by sequential nucleophilic addition and intramolecular esterification. The organocatalytic ring-opening polymerization (ROP) of these monomers with 1,5,7-triazabicyclo[4.4.0]-dec-5-ene (TBD) and 1,8-diazabicyclo[5.4.0]undecane-7-ene (DBU)/thiourea (TU) as the catalysts was investigated, and they could all be polymerized in a controlled manner under optimized conditions, affording well-defined poly(ester-amide)s (PEAs) (**P1–P5**) with tailored molar masses and narrow dispersities. The structures of these PEAs were characterized, confirming that the main-chain tertiary amide bonds existed as a mixture of *cis*/*trans* isomers. These PEAs are amorphous materials with high thermal stability ($T_{d,5\%}$: 260–301 °C) and side chain-dependent glass transition temperatures (T_gs) (62–138 °C). Polymer **P1** contains both a rigid benzene ring and a pyrrole ring in the backbone, being a PEA with the highest $T_{d,5\%}$ (301 °C) and T_g (138 °C). The TBD-catalyzed copolymerization of **M1** and *rac*-LA could generate a series of random copolymers with tunable and enhanced T_gs (52–96 °C) with increasing incorporation ratio of **M1** (0–51 mol%). Finally, These PEAs could be selectively and completely converted into their corresponding monomer precursors in alkaline aqueous solutions.

Introduction

Poly(ester-amide)s (PEAs) are an important family of degradable synthetic polymers with excellent thermal and mechanical properties. They have been widely investigated as biodegradable materials for various applications such as drug delivery carriers, scaffolds for tissue engineering, and so forth.[1–5] PEAs can be synthesized *via* condensation polymerization of bifunctional monomers or ring-opening polymerization (ROP) of cyclic monomers.[1,2,6] Although many different bifunctional monomers (*e.g.*, diacids, diols, amino acids, hydroxy acids, and amino alcohols) can be used to vary the polymer structures, the polycondensation usually proceeds slowly and shows poor control over the polymer molar mass and dispersity. Copolymerization of lactams and lactones has been used to prepare PEAs, but the difference of monomer reactivity leads to uncontrolled polymerization, and in most cases, it generates PEAs with ill-defined structures and low molar mass. The ROP of cyclic(ester-amide)s is a facile procedure to prepare well-defined PEAs with high molar masses. The mostly investigated cyclic(ester-amide) monomers are morpholine-2,5-dione derivatives (MDs) (Scheme 1(A)), which can be easily prepared from different α-hydroxy acids and α-amino acids.[7] The ROPs of MDs in many early reports were catalyzed by metal catalysts or enzymes, and the molar mass and dispersity of the obtained PEAs were poorly controlled.[7,8] With the rapid development of organic catalysts in the ROP of cyclic monomers,[9–12] the organocatalytic ROP of MDs under mild conditions has been achieved recently.[13–18] Typical organocatalysts include 1,5,7-triazabicyclo[4.4.0]-dec-5-ene (TBD) and 1,8-diazabicyclo[5.4.0]undecane-7-ene (DBU)/thioureas (TUs). Besides these six-membered MDs, Hocker and Li also synthesized other types of macrocyclic (ester-amide)s by the depolymerization of PEAs and a ring enlargement strategy.[19–21] These synthetic procedures are generally not straightforward. These monomers exhibit different ROP behavior depending on the ring size, and even for the polymerizable monomers, their ROPs should be carried out at high temperature. These harsh conditions inevitably accelerate transesterification, leading to ill-defined low molar mass PEAs.

Semi-aromatic polymers with aromatic structures in their backbones usually have improved materials properties, and

Beijing National Laboratory for Molecular Sciences, Key Laboratory of Polymer Chemistry and Physics of Ministry of Education, Center for Soft Matter Science and Engineering, College of Chemistry & Molecular Engineering, Peking University, Beijing 100871, China. E-mail: fsdu@pku.edu.cn, zcli@pku.edu.cn

† Electronic supplementary information (ESI) available: Synthesis and characterization of monomers, additional DSC and TGA curves, and NMR spectra, and additional data on the ROP of **M2**. See DOI: https://doi.org/10.1039/d2py00683a

This journal is © The Royal Society of Chemistry 2022

Published on 12 July 2022. Downloaded by Institute of Chemistry, CAS on 5/7/2026 9:22:57 AM.

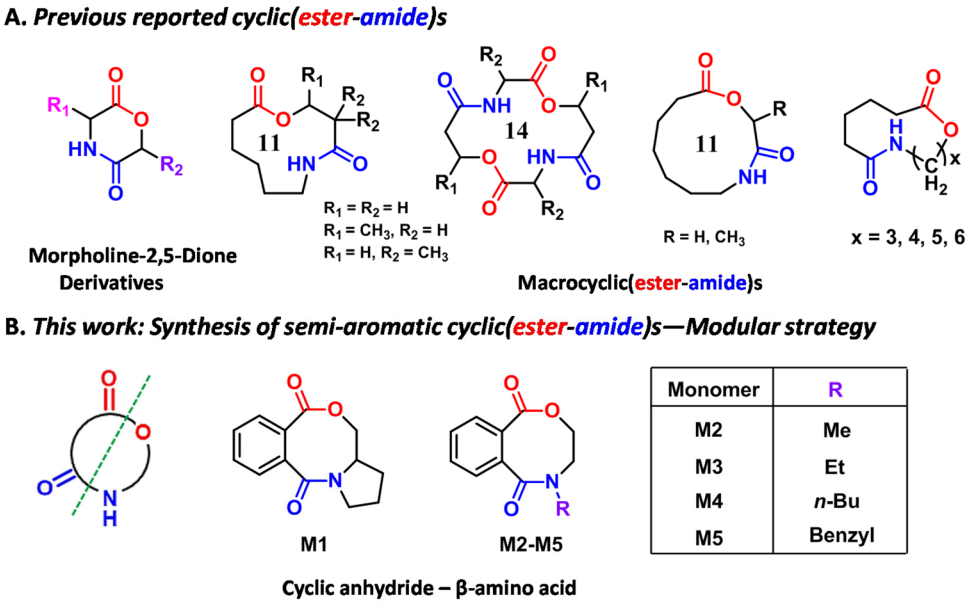

Scheme 1 (A) Previously reported cyclic(ester-amide)s for ROP: MDs and macrocyclic(ester-amide)s and (B) cyclic monomers synthesized *via* a modular strategy in this work.

some semi-aromatic polyesters such as poly(ethylene terephthalate) (PET) have been commercialized. Most of the semi-aromatic PEAs are synthesized by polycondensation.[1,2,22,23] Recently, the ring-opening alternating copolymerization (ROAP) of aziridines and phthalic anhydrides was explored as a new methodology to generate semi-aromatic PEAs, and the controllability of the ROAP was dependent on the structures of aziridines. The ROAP of the unsubstituted aziridine or the less nucleophilic *N*-alkyl aziridines with cyclic anhydrides generated uncontrolled products owing to the unavoidable zwitterionic side reactions.[24–26] Only the electrophilic *N*-sulfonyl aziridines were found to copolymerize with cyclic anhydrides in a controllable manner.[27] As far as we know, there is no report on the synthesis of semi-aromatic PEAs *via* the ROP of the corresponding cyclic (ester-amide)s. In this work, we intend to report a facile modular synthetic pathway for eight-membered cyclic (ester-amide)s starting from readily available phthalic anhydride (PA) and β-amino alcohols (**M1–M5**, Scheme 1B), investigate their organocatalytic ROP, and obtain a series of semi-aromatic PEAs with tunable and enhanced thermal stability while retaining their inherent degradability.

Experimental part

Materials

Phthalic anhydride (97%, Xilong Scientific), ethanolamine (99%, Xilong Scientific), L-(+)-prolinol (97%, Bidepharm), *N*-methylethanolamine (99%, Heowns Biochem), *N*-ethylethanolamine (95%, Konoscience), *N*-butylethanolamine (98%, Rhawn), *N*-benzylethanolamine (98%, Bidepharm), benzyl alcohol (H_2O < 30 ppm, J&K), 1*H*-benzotriazol-1-yloxytris(dimethylamino)phosphonium hexafluorophosphate (BOP reagent, 98%, Bidepharm), 1,8-diazabicyclo[5.4.0]undec-7-ene (DBU, 98%, J&K) and triazabicyclo [4.4.0]dec-5-ene (TBD, 98%, J&K) were purchased from commercial suppliers and used directly. Dichloromethane (DCM) and *N,N*-dimethylformamide (DMF) were purchased from J&K. 1-(3,5-Bis(trifluoromethyl)phenyl-3-cyclohexyl-2-thuourea) (TU) was synthesized according to a previously reported procedure.[28]

Measurements

^{1}H and ^{13}C NMR spectra were recorded on a Bruker Avance 400 MHz or 500 MHz spectrometer using tetramethylsilane as the reference. Electrospray ionization mass spectra (FT-MS) were recorded on a Bruker Solarix XR Fourier transform mass spectrometer in the positive ion mode with high resolution. Size exclusion chromatography (SEC) measurements of polymers **P1–P5** were performed on a system equipped with an isocratic pump (Model 1100, Agilent Technology, Santa Clara, CA), a DAWN HELEOS 9-angle laser light scattering (MALLS) detector (Wyatt Technology, Santa Barbara, CA), and an Optilab rEX refractive index detector (Wyatt Technology, Santa Barbara, CA). The temperature of both the refractive index and MALLS detectors was 25 °C. Separations were performed using serially connected size exclusion columns (500, 10^3, 10^4, and 10^5 Å Phenogel columns, 5 μm, 7.8 × 300 mm, Phenomenex, Torrance, CA) at a flow rate of 1.0 mL min^{-1} and 50 °C using DMF containing 0.1 M LiBr as the mobile phase. The calibration was made against linear poly(methyl methacrylate) (PMMA) standards, and the data were collected and processed

Published on 12 July 2022. Downloaded by Institute of Chemistry, CAS on 5/7/2026 9:22:57 AM.

with the Wyatt Astra software. SEC experiments of copolymers **C1–C5** were performed on a Waters system equipped with a Waters 1525 binary HPLC pump, a Waters 2414 refractive index detector, and three Waters Styragel HT columns (HT2, HT3, and HT4) thermostated at 35 °C. THF was used as the eluent at a flow rate of 1.0 mL min^{-1}. The calibration was made against a series of polystyrene standards. The data were collected and processed with Breeze software. Thermal gravimetric analysis (TGA) was performed on a Q600-SDT thermogravimetric analyzer (TA Co. Ltd). Polymer samples were heated from 50 °C to 600 °C at a heating rate of 10 °C min^{-1} under a nitrogen flow of 100 mL min^{-1}. Decomposition onset temperatures ($T_{d,5\%}$) of the polymers were defined at a 5% weight loss. Differential scanning calorimetry (DSC) was performed on a TA Q100 differential scanning calorimeter. Polymer samples were heated from −50 °C to 200 °C at a heating/cooling rate of 10 °C min^{-1} under a nitrogen flow of 50 mL min^{-1}. Data of the endothermic thermograms were recorded from the second scan and analyzed with TA Universal Analysis software.

Synthesis of monomers

Detailed synthetic procedures and characterization of monomers **M1–M5** are provided in the ESI.†

ROP studies

The ROP of **M1** catalyzed by TBD was described as a representative example (Table 1). In a N2-filled glovebox, monomer **M1** (231 mg, 1.0 mmol) was dissolved in DMF (0.30 mL) in a 2 mL vial containing a micro stir bar, and then 50 μL of BnOH solution (1.0 M in DMF) and 50 μL of TBD solution (1.0 M in DMF) were added to the vial successively. The mixture was stirred at 30 °C. After 5 min, excess benzoic acid solution in DMF was added to quench the reaction. The crude product was purified by three successive precipitations from diethyl ether and dried *in vacuo*. Polymer **P1a** was obtained as a white solid (202 mg, 89%).

The ROP of **M2** catalyzed by DBU/TU was described as a representative procedure of ROPs of **M2–M5** (Table 2, entry 1). In a N_2-filled glovebox, **M2** (205 mg, 1.0 mmol) and TU (18.5 mg, 0.05 mmol) were dissolved in DMF (0.3 mL) in a 2 mL vial containing a micro stir bar, and then 50 μL BnOH solution (1.0 M in DMF) and 50 μL DBU solution (1.0 M in DMF) were sequentially added to the vial. The mixture was stirred at 30 °C. After 0.5 h, the polymerization was quenched by adding excess benzoic acid solution in DMF. The crude product was purified by three successive precipitations from diethyl ether and dried *in vacuo*. Pure **P2a** was obtained as a white solid (170 mg, 83%). Polymers **P3–P5** were prepared by changing the amount of DBU/TU catalysts under similar conditions.

Alcoholysis of monomers and polymers

In an NMR tube, 20 mg of **P1a** (Table 1, $M_{n,SEC}$ = 5.2 kDa) was dissolved in 0.6 mL of MeOD-d_4, then a catalytic amount of TBD (10 wt% of **P1a**) was added, and the reaction mixture was placed in an oil bath at room temperature. At a specific time, the mixture was characterized by ^{1}H NMR. The experimental

Table 1 TBD-catalyzed ROP of **M1** [a]

Polymer	$[\mathbf{M}]_0/[TBD]/[I]_0$	Time (h)	Conv.[b] (%)	Yield[c] (%)	$M_{n,SEC}$[d] (kDa)	$Đ$[d]	DP[e]
P1a	20 : 1 : 1	5 min	>99	89	5.2	1.17	20.5
P1b	40 : 1 : 1	10 min	>99	95	11.0	1.08	52.4
P1c	80 : 1 : 1	2	97	90	15.1	1.12	89.1
P1d	120 : 1 : 1	37	>99	85	22.2	1.18	139.8
P1e	200 : 1 : 1	145	87	86	36.9	1.11	—[f]

[a] All the polymerizations were conducted at 30 °C in DMF ($[\mathbf{M1}]_0$ = 2.5 M) with BnOH as the initiator and TBD as the catalyst. [b] Determined by ^{1}H NMR (Fig. S6†). [c] Isolated yield. [d] Determined by SEC using DMF (containing 0.1 M LiBr) as the eluent and calibrated with PMMA standards. [e] Degree of polymerization of the purified **P1** polymers determined by ^{1}H NMR. [f] Not calculated due to very low signal intensity of the initiating benzyl ester in the purified polymer.

Table 2 DBU/TU-catalyzed ROP of **M2** [a]

Polymer	$[\mathbf{M}]_0/[DBU]/[TU]/[I]_0$	Time (h)	Conv.[b] (%)	Yield[c] (%)	$M_{n,SEC}$[d] (kDa)	$Đ$[d]	DP[e]
P2a	20 : 1 : 1 : 1	0.5	>99	83	4.6	1.12	19.9
P2b	40 : 1 : 2 : 1	1	>99	80	8.2	1.04	36.8
P2c	80 : 1 : 4 : 1	6	92	84	15.9	1.05	75.7
P2d	120 : 1 : 5 : 1	14	91	85	22.2	1.04	102.2
P2e	200 : 3 : 5 : 1	39	80	79	40.0	1.05	—[f]

[a] All polymers were generated in DMF ($[\mathbf{M}]_0$ = 2.5 M) with BnOH as the initiator and DBU/TU as the catalyst at 30 °C. [b] Determined by ^{1}H NMR (Fig. S10†). [c] Isolated yield. [d] Determined by SEC using DMF (containing 0.1 M LiBr) as the eluent and calibrated with PMMA standards. [e] Degree of polymerization of the purified **P2** samples determined by ^{1}H NMR. [f] Not calculated due to very low signal intensity of the initiating benzyl ester in the purified polymer.

 This journal is © The Royal Society of Chemistry 2022

Published on 12 July 2022. Downloaded by Institute of Chemistry, CAS on 5/7/2026 9:22:57 AM.

procedure was the same for the alcoholysis of **M1**, **M2**, and **P2a**.

Preparation of compounds D1 and D2

In a 20 mL round bottom flask, 400 mg of **P1a** and 10 wt% TBD were dissolved in MeOH (5 mL), and the reaction mixture was vigorously stirred at room temperature for 24 h. The reaction mixture was then concentrated *in vacuo* and further purified by flash column chromatography (EtOAc/PE = 1/1, v/v). The degradation product **D1** was obtained as a colorless oil. The experimental procedure was the same for the preparation of compound **D2**.

Copolymerization of M1 and *rac*-LA

The synthetic procedure of copolymer **C5** was described as a representative protocol. In a N2-filled glovebox, monomer **M1** (231 mg, 1.0 mmol) and *rac*-LA (144 mg, 1.0 mmol) were dissolved in DCM (0.8 mL) in a 4 mL vial containing a micro stir bar, and then 100 μL of BnOH solution (0.20 M in DCM) and 100 μL of TBD solution (0.20 M in DCM) were added to the vial successively. The mixture was stirred at 30 °C. At a specific time, 40 μL of the reaction solution was taken out and transferred into an NMR tube, and quickly quenched by adding an excess benzoic acid solution. After removing the solvent *in vacuo*, the residue was re-dissolved in $CDCl_3$ for ^{1}H NMR measurements. After 40 min, the polymerization reached complete monomer conversion, and excess benzoic acid solution was then added to quench the reaction. The crude product was purified by three successive precipitations from diethyl ether and dried *in vacuo*. Copolymer **C5** was obtained as a white solid (255 mg). Other copolymers **C1–C4** were prepared in a similar way by varying the feed ratio of $[\mathbf{M1}]_0/[rac\text{-LA}]_0$. The yields of these copolymers are 60% (**C1**), 62% (**C2**), 67% (**C3**), 78% (**C4**), and 68% (**C5**), respectively.

Hydrolytic degradation of polymers

In an NMR tube, 5 mg of **P1a** (Table 1) was dissolved in 0.4 mL of DMSO-d_6. Then, NaOD in D_2O (40 wt%, 6 μL) and D_2O (30 μL) were charged prior to ^{1}H NMR measurements. The NMR tube was incubated at 30 °C. At the prescribed reaction time (24 h), the mixture was characterized by ^{1}H NMR. The experimental procedure was the same for the hydrolysis of **P2a**.

Results and discussion

Monomer synthesis

The ring size of a monomer greatly influences its ROP behavior. Generally, the polymerization of small-ring lactones is enthalpy-driven by the release of the ring strain of the monomer.[29,30] Five-membered γ-BL is less polymerizable under ambient conditions due to its thermodynamic stability, but can be polymerized in bulk with highly active catalysts at low temperature.[31] To date, PEAs have been synthesized from the ROPs of MDs and eleven to fourteen-membered macrocyclic monomers.[19–21,32–37] Eight-membered cyclic(esteramide)s have been less explored.[38–40] The reported synthetic routes of these monomers were tedious and the starting materials were not readily available. In addition, the ROPs of these cyclic compounds have not been investigated.

To access a wide variety of eight-membered cyclic(esteramide)s, we developed a simple two-step approach starting from commercially available phthalic anhydride (PA) and β-amino alcohols (Scheme 2). The latter reagents can be readily synthesized by the reduction of amino acids.[41] To demonstrate the feasibility of this strategy, we chose five β-amino alcohols, and all of them reacted rapidly with PA in DMF at room temperature. The obtained hydroxy acids were converted into **M1–M5** by the subsequent dehydrating cyclization in anhydrous THF.[42] These five monomers were obtained in moderate yields, and their structures were characterized by ^{1}H NMR, ^{13}C NMR, and FT-MS (Fig. S1–S5†). It should be noted that the amide linkages in **M1–M5** were all tertiary amides. When we used primary β-amino alcohols (such as ethanolamine and 2-amino-1-propanol) as starting materials, the obtained products were *N*-substituted phthalimides other

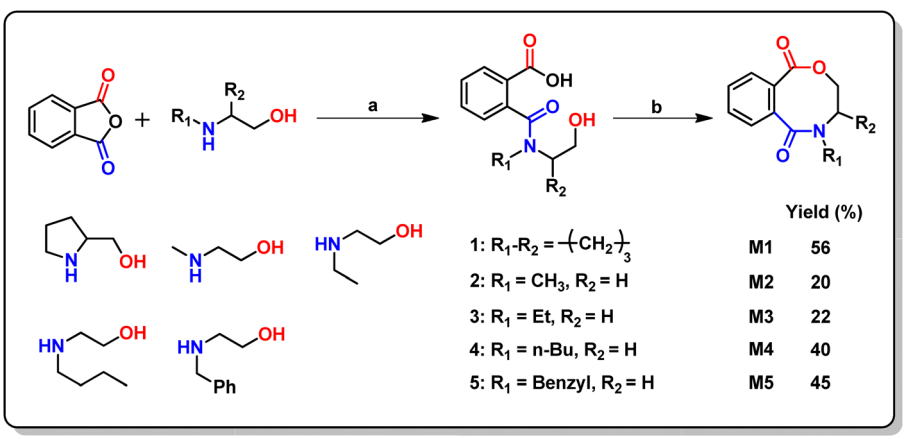

Scheme 2 Monomer synthesis. Reagents and conditions: (a) DMF, RT, 10 min and (b) 1.1 equiv. BOP reagent, 1.3 equiv. Et_3N, THF, RT, 2 h.

Published on 12 July 2022. Downloaded by Institute of Chemistry, CAS on 5/7/2026 9:22:57 AM.

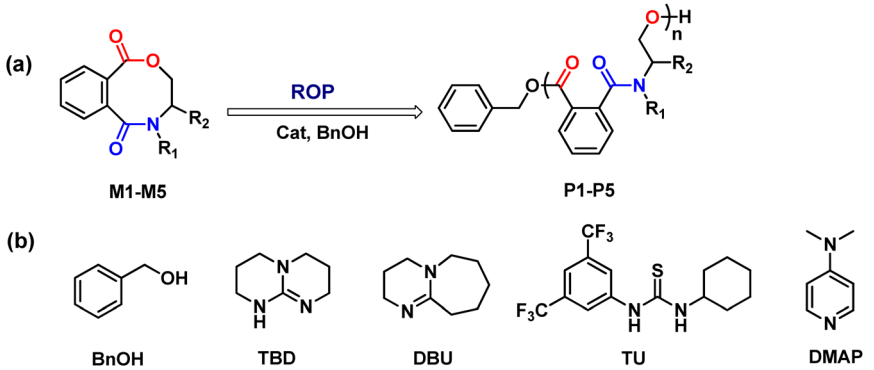

Scheme 3 (a) Organocatalytic ROP of **M1–M5**; (b) chemical structures of BnOH, TBD, DBU, TU, and DMAP.

than the desired cyclic monomers with secondary amide linkages.[43] Collectively, a novel class of eight-membered cyclic (ester-amide)s can be prepared by this efficient synthetic route from commercially available materials.

ROP of M1

Organobase catalysts such as TBD and DBU/TU have been proved to be efficient catalysts for the ROP of six-membered MDs.[13–17,21] On the basis of insights from these previous studies, we first performed the TBD-catalyzed ROP of **M1** under different conditions (Scheme 3). THF was initially used as the solvent, but the low solubility of the formed polymer **P1** limited monomer conversion and caused an increase of polymer molar mass. Then, we changed the solvent to DMF. TBD was reported to simultaneously activate the lactone monomer and the –OH of the initiator/propagating species,[44] and the monomer activation efficiency might be retarded by the carbonyl group of DMF. To our delight, TBD can effectively catalyze the ROP of **M1** in DMF to afford PEAs. Under the conditions of $[\mathbf{M1}]_0/[\mathrm{BnOH}]_0/[\mathrm{TBD}]_0$ = 20/1/1, $[\mathbf{M1}]_0$ = 2.5 mol L^{-1}, and 30 °C, **M1** was almost completely polymerized in 5 min, and the obtained polymer exhibited a symmetric unimodal SEC trace with a low $Đ$ value of 1.17 (Table 1). By varying the feed ratio of **M1** to BnOH (M/I) from 20/1 to 200/1, and prolonging the polymerization time from 5 min to 145 h, a series of **P1** with different molar masses and low $Đ$ values (<1.2) were synthesized (Table 1). The SEC traces of all these polymers were unimodal, and there was an approximately linear relationship between $M_{n,SEC}$ and DP, suggesting a controllable ROP process (Fig. 1). Polymer **P1e** with the highest molar mass ($M_{n,SEC}$ = 36.9 kDa) was obtained in 86% yield (Table 1).

Fig. 2a shows the representative ^{1}H NMR spectrum of the purified polymer **P1a** (Table 1). The proton signals of benzyl ester –CH_2– (~5.3 ppm) at the initiating chain end was clearly observed. According to the integration ratio of the aromatic protons at ~7.8–8.2 ppm (signals 1 + 1′) to the benzyl methylene protons at 5.3 ppm, the degree of polymerization (DP) of **P1a** was determined to be 20.5. This value agrees well with the theoretical value calculated from the monomer to initiator ratio, and supports the linear structure of **P1a**. Moreover, because of the occurrence of *cis–trans* isomerization of the tertiary amides in the polymer backbone, there are two sets of signals for some protons, for instance, peaks 1 *vs.* 1′, and peaks 8 + 9 *vs.* 8′ + 9′. A similar phenomenon is usually observed for the tertiary amides with different substituents, in which the isomeric ratio of *cis* to *trans* isomers is dependent on the nature and size of the *N*-substituents.[45–49] To confirm

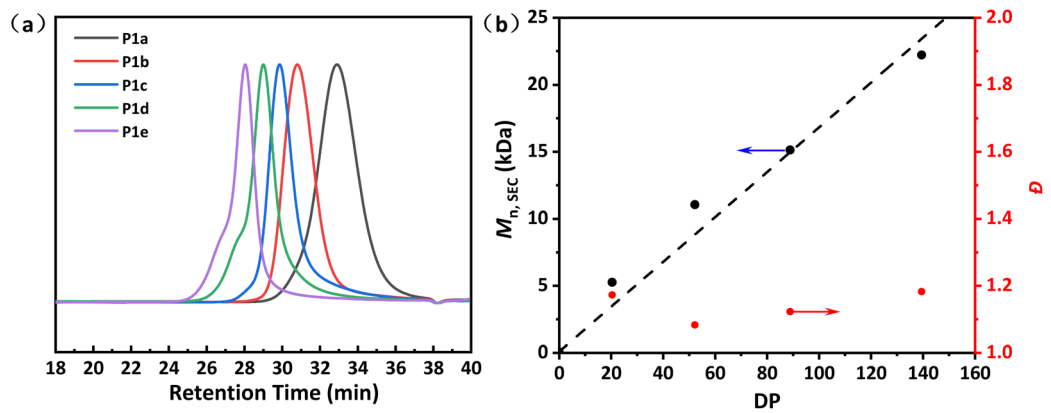

Fig. 1 Characterization of **P1** (Table 1): (a) SEC traces; (b) plot of $M_{n,SEC}$ and $Đ$ *vs.* degree of polymerization (DP).

 This journal is © The Royal Society of Chemistry 2022

Published on 12 July 2022. Downloaded by Institute of Chemistry, CAS on 5/7/2026 9:22:57 AM.

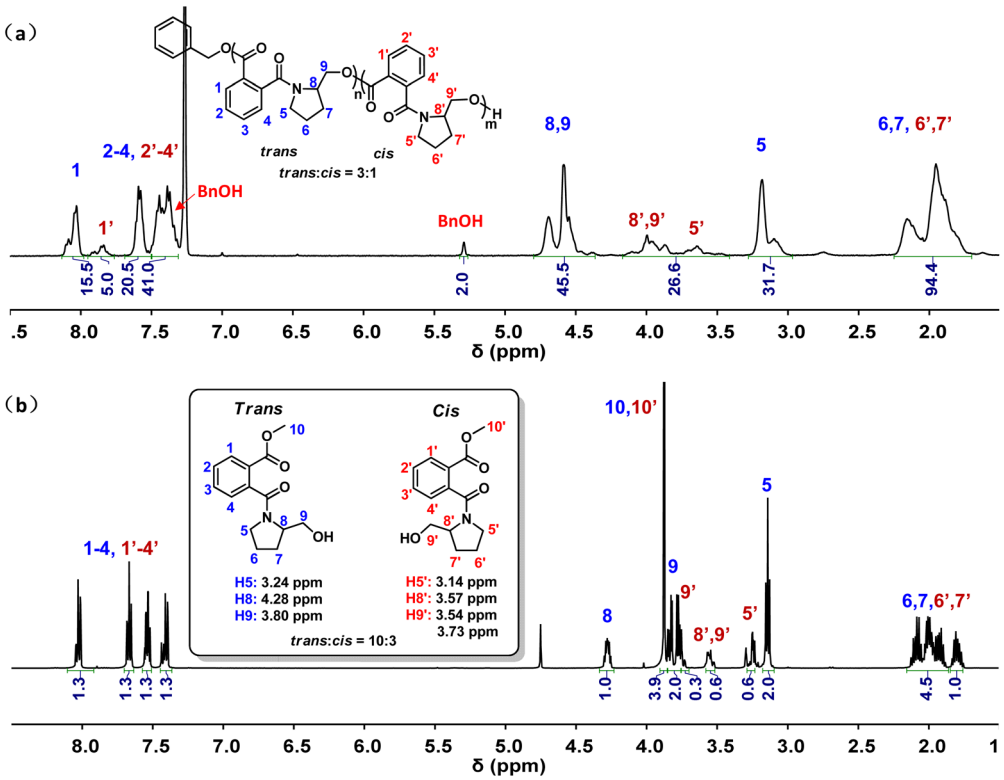

Fig. 2 (a) ^{1}H NMR spectrum of **P1a** in $CDCl_3$; (b) ^{1}H NMR spectrum of the degradation product **D1** in MeOD-d_4. The *trans* to *cis* ratio is calculated from the intensity of peaks 5 and 5′ in both spectra.

this assumption, **M1** and **P1a** were subjected to alcoholysis in deuterated methanol in the presence of TBD. Both reactions generated the same products (Fig. S7†), thus excluding the possible side reactions during the polymerization process. We further prepared the pure degradation product **D1** *via* the TBD-catalyzed alcoholysis of **P1a** in methanol, and analyzed its structure by ^{1}H/^{13}C NMR and ^{1}H–^{13}C HSQC NMR (Fig. 2b, S8 and S9†). These spectra indicate clearly that **D1** contains both *trans* and *cis* isomers, in which the chemical shifts of the proton and carbon atoms adjacent to the nitrogen atom are drastically different. By comparing the peak intensities of protons 5 and 5′, the ratio of *trans* to *cis* isomers of **D1** was determined to be 10 : 3, which is close to that (9 : 3) of the polymer **P1a** (Fig. 2). Similarly, the *trans* and *cis* isomer ratios in other **P1** samples were measured, and the percent content of the *trans* isomer was in the range of 75% to 79%, being almost independent of the molar mass of the polymers.

ROP of M2–M5

Next, the ROP of **M2** was also carried out using TBD as the catalyst. Similar to the ROP of **M1**, the ROP of **M2** also proceeds very quickly, but it is not well-controlled. The molar masses of the obtained polymers ($M_{n,SEC}$) from different **M2**/I ratios were largely deviated from the theoretical values ($M_{n,calcd}$) based on monomer conversions, and the dispersities were also large ($Đ$ = 1.36–1.70) (Table S1†). The different ROP behaviors of **M1** and **M2** were attributed to the difference of polymer structures. For polymer **P1**, the rigidity of the steric pyrrolidine ring could further reduce the backbone flexibility, suppressing the undesired transesterification side reactions during the TBD-catalyzed ROP of **M1**.

To achieve a more controllable ROP of **M2**, we screened other organic base catalysts, including DBU, DMAP, and DBU/TU. DMAP did not exhibit any catalytic activity mainly because of its weak basicity.[28] Both DBU and DBU/TU could successfully catalyze the ROP of **M2**, affording polymer **P2** with a narrow dispersity ($Đ$ < 1.1). Since TU could act as a cocatalyst to further improve the organobase-catalyzed ROP of cyclic ester monomers, lactones, and reduce the transesterification side reactions,[9,12,28,44,50] we used a DBU/TU binary system for the ROP of **M2–M5** in the following sections.

The DBU/TU-catalyzed ROP of **M2** was also performed with five different $[\mathbf{M2}]_0/[\mathrm{BnOH}]_0$ ratios (Table 2). To better control the ROP, more TU was used for polymerization with a high $[\mathbf{M}]_0/[\mathrm{I}]_0$ ratio. It took a long time to achieve high monomer conversion, which is similar to the ROP of **M1**. All the obtained **P2** samples possess narrow dispersities ($Đ$ < 1.2) and exhibit a good correlation between $M_{n,SEC}$ and DP (Fig. 3), and the highest molar mass was up to 40 kDa.

Fig. 4a shows the ^{1}H NMR spectrum of the isolated **P2a** (Table 2), in which the methylene proton signal at ~5.3 ppm of the initiating benzyl ester is clearly observable. Again, we observed two sets of proton signals assigned to *trans* and *cis* isomers of the repeating units, which can be supported by

Published on 12 July 2022. Downloaded by Institute of Chemistry, CAS on 5/7/2026 9:22:57 AM.

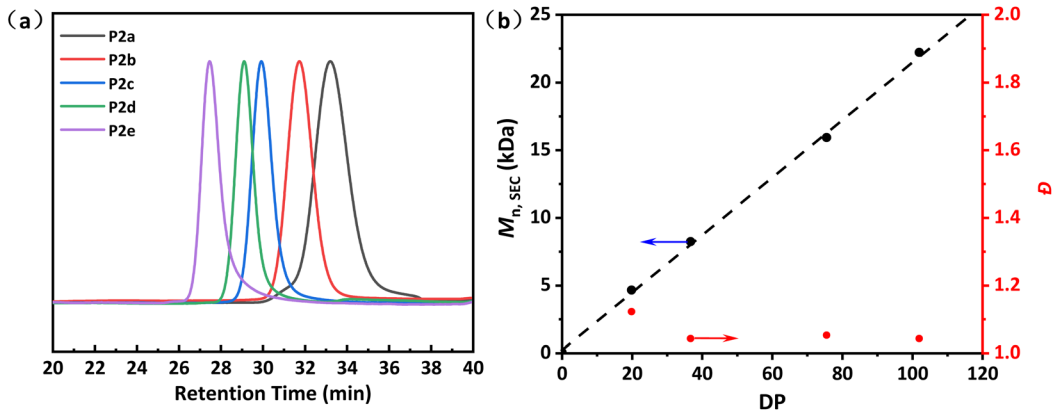

Fig. 3 Characterization of **P2**: (a) SEC traces and (b) plot of $M_{n,SEC}$ and $Đ$ *vs.* degree of polymerization (DP).

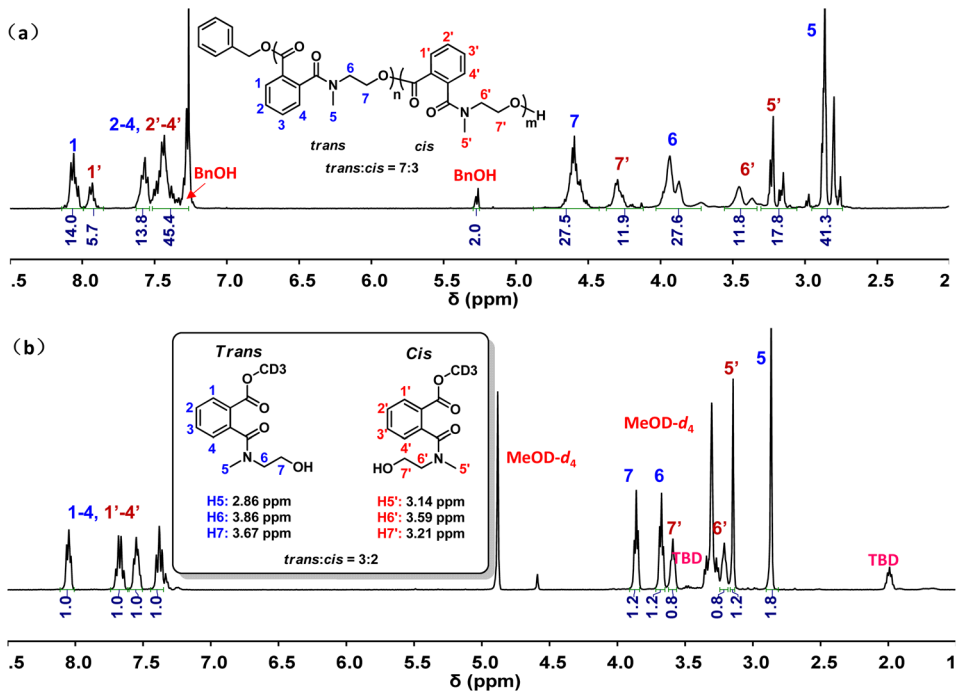

Fig. 4 (a) ^{1}H NMR spectrum of **P2a** (Table 2) in $CDCl_3$ and (b) ^{1}H NMR spectrum of the degradation product **D2** in MeOD-d_4. The *trans* to *cis* ratio is calculated from the intensity of peaks 7 and 7′ in both spectra.

comparing the alcoholysis products of **P2a** and **M2** in Fig. S11.† On the basis of the intensity of peak 1 (8.15–8.0 ppm) and peak 1′ (8.0–7.86 ppm), the ratio of *trans* to *cis* isomers of **P2a** was determined to be 7 : 3, which is lower than that (9 : 3) of **P1a**. This means that the priority of *trans* to *cis* isomers in these PEA polymers is intensified by the steric pyrrolidine ring in the backbone. The *trans* to *cis* isomer ratio in **D2** (the alcoholyzed product of **P2a**) was found to be 3 : 2 (Fig. 4b), which is also much lower than that in **D1**.

The DBU/TU-catalyzed ROPs of **M3–M5** with BnOH as the initiator also proceeded smoothly in DCM at 30 °C, and two polymer samples were prepared for each monomer (Table 3). The low-molar-mass polymer samples were used to verify their chemical structures, while the high-molar-mass ones were used to characterize their properties. All the six polymer samples had low dispersities ($Đ$ < 1.10), and the calculated DPs of the low-molar-mass polymer samples (**P3a**, **P4a**, and **P5a**) were close to their corresponding feed ratios of $[\mathbf{M}]_0/[\mathrm{BnOH}]_0$ (Fig. S12†).

Thermal properties of PEAs

Thermal gravimetric analysis (TGA) was conducted on the polymer samples to evaluate their thermal stabilities. As shown in Fig. S14,† the decomposition temperatures ($T_{d,5\%}$) of **P1** and **P2** increased with the increase of molar mass of the polymers, and remained virtually unchanged when the molar

 This journal is © The Royal Society of Chemistry 2022

Published on 12 July 2022. Downloaded by Institute of Chemistry, CAS on 5/7/2026 9:22:57 AM.

Table 3 DBU/TU-catalyzed ROP of **M3–M5** [a]

Polymer	$[M]_0/[DBU]/[TU]/[BnOH]_0$	Time (h)	Conv.[b] (%)	Yield[c] (%)	$M_{n,SEC}$[d] (kDa)	$Đ$[d]	DP[e]
P3a	20 : 1 : 1 : 1	0.5	>99	69	4.9	1.06	20.3
P3b	200 : 3 : 5 : 1	43	82	82	25.9	1.09	—[f]
P4a	20 : 1 : 1 : 1	0.5	>99	64	5.3	1.06	22.3
P4b	200 : 3 : 5 : 1	43	89	89	26.2	1.10	—[f]
P5a	20 : 1 : 1 : 1	0.5	>99	63	5.0	1.07	19.7
P5b	200 : 3 : 5 : 1	43	>99	82	33.9	1.06	—[f]

[a] All the polymerizations were conducted at 30 °C in DCM ($[M]_0$ = 2 M) with BnOH as the initiator and DBU/TU as the catalyst. [b] Determined by ^{1}H NMR spectroscopy. [c] Isolated yield. [d] Determined by DMF (containing 0.1 M LiBr) SEC and calibrated with the PMMA standard. [e] Degree of polymerization of the purified polymers determined by ^{1}H NMR. [f] Not calculated due to very low signal intensity of the initiating benzyl ester in the purified polymer.

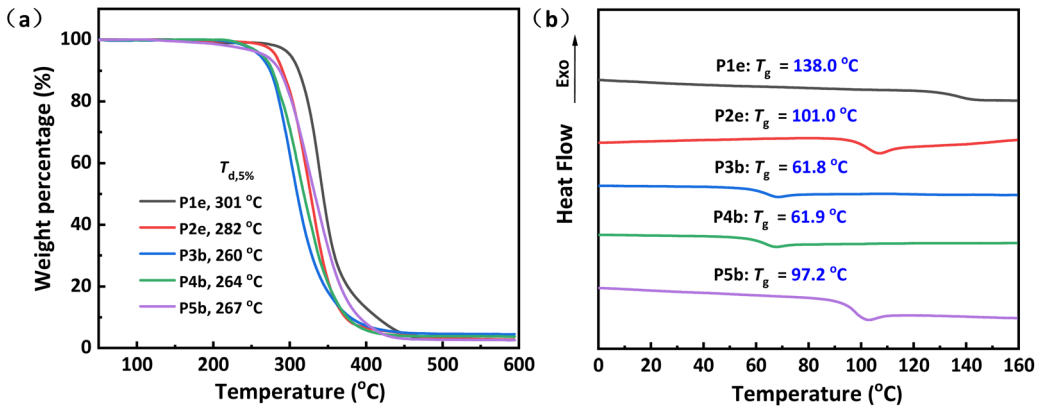

Fig. 5 Thermal properties of **P1–P5**: (a) TGA and (b) DSC thermograms.

masses reached ~8 kDa (**P1**, 300 °C, **P2**, 282 °C). The $T_{d,5\%}$ of the high-molar-mass **P3–P5** was in the range of 260 °C to 267 °C, revealing that **P1** is more thermally stable than **P2–P5** (Fig. 5a).[51]

Differential scanning calorimetry (DSC) was performed to measure the glass transition temperatures (T_g) of these polymers. They are all amorphous materials with tunable T_g. Taking **P1** and **P2** as examples, their T_gs also increased with the increase of their molar masses (Fig. S15†). Among all the five polymer samples, **P1** exhibited the highest T_g (138 °C) owing to the stiffness in the polymer backbone imparted by the rigid pyrrolidine rings.[52–54] As the *n*-alkyl side chain length of **P2–P4** became longer (methyl, ethyl, and *n*-butyl), the T_g decreased dramatically from 101.0 °C for **P2** to 61.8 °C for **P3**, and to 61.9 °C for **P4** (Fig. 5b), a phenomenon commonly observed in alkyl polymethacrylates.[55] Polymer **P5** had a high T_g of 97.2 °C, which was mainly attributed to the pendant bulky benzyl groups.

Copolymerization of M1 and *rac*-LA

Lactide (LA) is known to polymerize rapidly using TBD as the catalyst,[56] and the reported T_g of polylactide (PLA) is in a temperature range of 35–60 °C, which greatly limits the potential application of amorphous PLA.[57] Copolymerization is a well-established strategy to create copolymers with varied T_gs.[15,57,58] To increase the T_g of PLA-based materials, we examined the copolymerization of *rac*-LA and **M1**. We first confirmed that the TBD-catalyzed ROP of *rac*-LA ($[rac\text{-}LA]_0 : [BnOH]_0 : TBD$ = 100 : 1 : 1) in DCM at 30 °C could reach complete conversion in 5 min, affording a PLA sample with a molar mass up to 27.4 kDa. We then conducted the copolymerization of *rac*-LA and **M1** under the same conditions ($([rac\text{-}LA]_0 + [\mathbf{M1}]_0) : [BnOH]_0 : TBD$ = 100 : 1 : 1), and five copolymers **C1–C5** were produced by varying the feed ratios (Table 4). Copolymerizations with higher **M1** feed ratios require longer time to reach high monomer conversions. The incorporation ratios of **M1** in the copolymers were calculated from the corresponding ^{1}H NMR spectra of **C1–C5** (Fig. S16†), which are consistent with the feed ratios.

The copolymerization process was followed by ^{1}H NMR for the synthesis of copolymer **C5**, and the time-dependent ^{1}H NMR spectra are shown in Fig. 6. Clearly, *rac*-LA polymerized preferentially at the beginning and reached full conversion in 50 s, while only a small fraction of **M1** was incorporated. Two sequences, LA–LA and LA–**M1**, existed at 5.10–5.25 ppm and 5.25–5.46 ppm, respectively (marked as red and blue dots in Fig. 6), and the signal intensity of LA–**M1** was much lower than that of LA–LA. With the progress of the polymerization,

Published on 12 July 2022. Downloaded by Institute of Chemistry, CAS on 5/7/2026 9:22:57 AM.

Table 4 Synthesis and characterization of PLA and copolymers **C1–C5** [a]

(Co)polymer	Feed ratio [b] (%)		Time (min)	**M1** [c] (%)	M_n [d] (kDa)	$Đ$ [d]	$T_{d,5\%}$ [e] (°C)	T_g [f] (°C)	$T_{g,fox}$ [g] (°C)
	M1	*rac*-LA							
PLA	0	100	5	0	27.4	1.34	295	51.9	—
C1	10	90	10	10.1	23.7	1.39	258	56.3	57.5
C2	20	80	20	19.2	20.7	1.39	236	62.9	63.0
C3	30	40	20	31.2	19.4	1.53	243	74.1	71.0
C4	40	60	20	40.8	19.0	1.47	259	83.2	78.1
C5	50	50	40	51.2	18.1	1.39	282	95.7	86.6

[a] All the copolymerizations were conducted in DCM at 30 °C in a glove box under N_2 using BnOH as the initiator and TBD as the catalyst, ($[\mathbf{M1}]_0$ + $[LA]_0$)/$[BnOH]_0$/$[TBD]$ = 100/1/1, $[\mathbf{M}]_0$ = 2 M, and quenched when both monomers reached complete conversion. [b] Feed molar ratio. [c] Determined by ^{1}H NMR spectroscopy. [d] Determined by SEC using THF as the eluent and PS standards. [e] Determined by TGA. [f] Determined by DSC. [g] Calculated according to the Fox equation: $1/T_{g,fox} = \omega_1/T_{g,PLA} + \omega_2/T_{g,p1}$, where ω_1 and ω_2 represent the weight fraction of **LA** and **M1**, respectively.

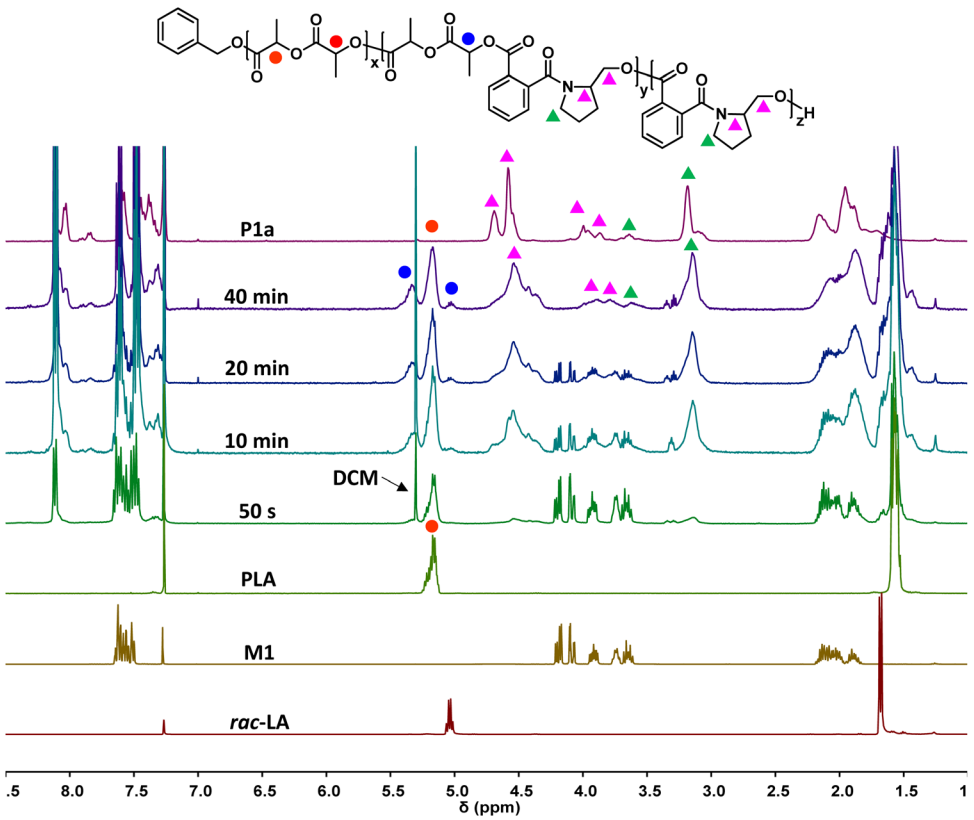

Fig. 6 Time-dependent ^{1}H NMR spectra of the copolymerization mixture of **M1** and *rac*-LA.

the conversion of **M1** increased and reached over 95% after 40 min. On the basis of this polymerization process, it is expected that a tapered block copolymer, PLA-*b*-**PM1**, may be generated. However, it does not seem to be the case on comparing the ^{1}H NMR spectra of PLA, **PM1**, and **C5**. The intensity of the LA–**M1** sequences in the ^{1}H NMR spectra increased steadily with the increase in the conversion of **M1** after LA had been depleted, suggesting a random-like structure of copolymer **C5**. This was supported by the fact that TBD, a well-known highly active catalyst for the ROP of cyclic esters, has been demonstrated to catalyze polyester transesterification at high monomer conversion.[44] The transesterification process was further evidenced by the large dispersities of copolymers **C1–C5**; moreover, by changing the feed ratio of **M1** to *rac*-LA from 10 : 90 to 50 : 50, the fractions of the **M1**–LA or LA–**M1** sequences increased from 8% to 37% (Fig. S16†). Thus, we proposed a possible copolymerization diagram of *rac*-LA and **M1** as shown in Fig. S17.† At the beginning, *rac*-LA was depleted

 This journal is © The Royal Society of Chemistry 2022

Published on 12 July 2022. Downloaded by Institute of Chemistry, CAS on 5/7/2026 9:22:57 AM.

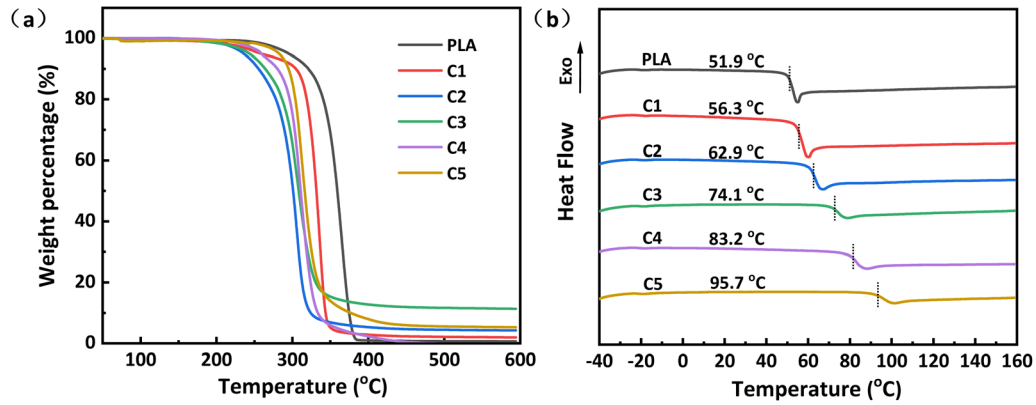

Fig. 7 Thermal properties of PLA and **C1–C5**: (a) TGA and (b) DSC thermograms.

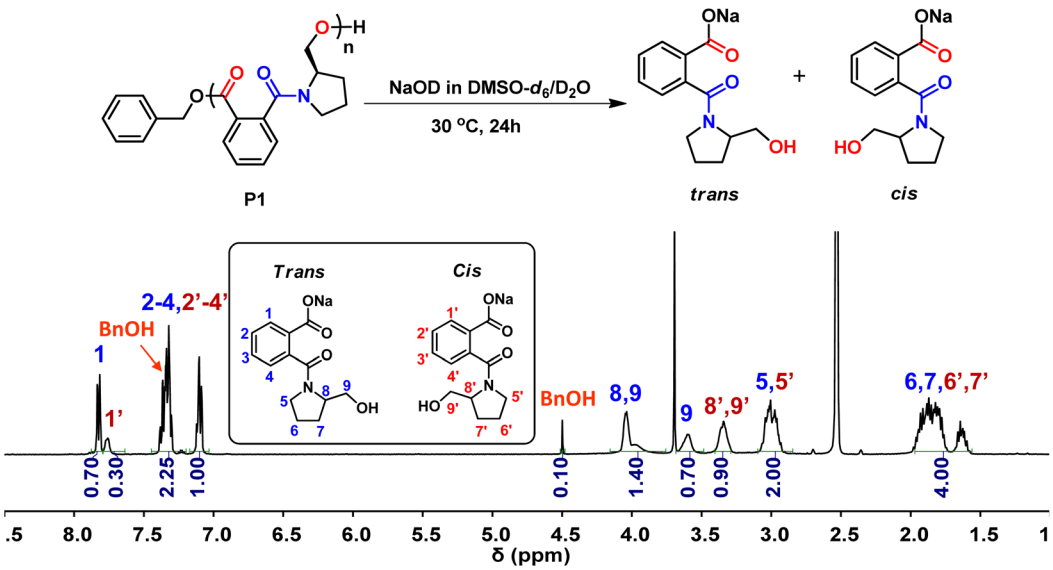

Fig. 8 ^{1}H NMR spectrum of the hydrolysis degradation product of **P1a** in DMSO-d_6.

very quickly, forming predominantly PLA homopolymers. Thereafter, monomer **M1** was added to the PLA chain ends, forming more nucleophilic primary alcohol end groups, which could initiate the ROP of **M1** and participate in transesterification. These two processes then occurred concurrently until monomer **M1** was completely consumed, resulting in the formation of a random-like copolymer of *rac*-LA and **M1**.

The thermal properties of **C1–C5** were investigated by TGA and DSC (Fig. 7), and the results are listed in Table 4. The TGA thermograms of PLA and **C1–C5** revealed that the incorporation of **M1** into PLA decreased the decomposition temperatures. However, there was no clear relationship between the composition and $T_{d,5\%}$ of the copolymers, which might be due to the complicated sequential and conformational structures of the copolymer chains.[59] These five copolymers are amorphous materials with their T_g being 56.3, 62.9, 74.1, 83.2, and 95.7 °C, respectively. These T_g values increased with the increasing incorporation ratio of **M1**, and they are close to the theoretical values calculated from the Fox equation (Table 4), further manifesting the random sequence of the copolymers.

Polymer degradation

Chemical recycling of polymers into monomers or monomer precursors offers a feasible solution to reduce fossil fuel use and relieve the environment pressure caused by the accumulation of plastic waste.[60–64] PEAs contain both ester and amide linkages in their backbones, and they are expected to chemically degrade into small molecules with either alkaline or acidic catalysts through the hydrolysis of the ester bonds. Degradation of **P1a** (Table 1) and **P2a** (Table S1†) was performed in DMSO-d_6/D_2O at 30 °C using NaOD as the catalyst. Fig. 8 shows the typical ^{1}H NMR spectrum of polymer **P1a** after 24 h. The proton signals of **P1** completely disappeared,

Published on 12 July 2022. Downloaded by Institute of Chemistry, CAS on 5/7/2026 9:22:57 AM.

and the emerging degradation product was a mixture of *cis*/*trans* isomers of the monomer precursor. The amide bonds remained intact under these basic hydrolysis conditions. Polymer **P2a** could also be degraded into its monomer precursor under similar conditions (Fig. S18†). These degradation products could be transformed into monomers **M1** and **M2** *via* intramolecular esterification.

Conclusion

In summary, we developed a simple synthetic method for five eight-membered cyclic(ester-amide) monomers from easily accessible phthalic anhydride and β-amino alcohols. Controlled ROP of **M1–M5** with organocatalysts was achieved, and a series of new semi-aromatic PEAs were prepared. These PEAs exhibit good thermal stability ($T_{d,5\%}$: 260–301 °C), and are amorphous materials with variable T_gs (62–138 °C). Polymer **P1** contains both a rigid benzene ring and a pyrrole ring in the backbone, possessing the highest $T_{d,5\%}$ and T_g. A series of random copolymers of **M1** and *rac*-LA were prepared by the TBD-catalyzed copolymerization of the two monomers. Their T_gs could be increased from 52 to 96 °C by increasing the incorporation ratio of **M1** in the copolymers to 51%. Finally, we demonstrated the controlled degradation of these PEAs by conducting the base-catalyzed hydrolysis of **P1** and **P2**. The combination of easily accessible starting materials, simple monomer synthetic procedures, controllable ROP of the cyclic monomers, and tunable polymer properties make this method an appealing route to semi-aromatic PEAs.

Conflicts of interest

There are no conflicts to declare.

Acknowledgements

This work was financially supported by the National Natural Science Foundation of China (No. 21871014).

References

1 M. Winnacker and B. Rieger, *Polym. Chem.*, 2016, **7**, 7039–7046.
2 A. C. Fonseca, M. H. Gil and P. N. Simoes, *Prog. Polym. Sci.*, 2014, **39**, 1291–1311.
3 H. Sun, F. Meng, A. A. Dias, M. Hendriks, J. Feijen and Z. Zhong, *Biomacromolecules*, 2011, **12**, 1937–1955.
4 A. Rodriguez-Galan, L. Franco and J. Puiggali, *Polymers*, 2011, **3**, 65–99.
5 S. Han and J. Wu, *Biomacromolecules*, 2022, **23**, 1892–1919.
6 A. Basu, K. R. Kunduru, J. Katzhendler and A. J. Domb, *Adv. Drug Delivery Rev.*, 2016, **107**, 82–96.
7 Y. Feng and J. Guo, *Int. J. Mol. Sci.*, 2009, **10**, 589–615.
8 Y. Feng, J. Lu, M. Behl and A. Lendlein, *Macromol. Biosci.*, 2010, **10**, 1008–1021.
9 W. N. Ottou, H. Sardon, D. Mecerreyes, J. Vignolle and D. Taton, *Prog. Polym. Sci.*, 2016, **56**, 64–115.
10 C. Thomas and B. Bibal, *Green Chem.*, 2014, **16**, 1687–1699.
11 M. K. Kiesewetter, E. J. Shin, J. L. Hedrick and R. M. Waymouth, *Macromolecules*, 2010, **43**, 2093–2107.
12 N. E. Kamber, W. Jeong, R. M. Waymouth, R. C. Pratt, B. G. G. Lohmeijer and J. L. Hedrick, *Chem. Rev.*, 2007, **107**, 5813–5840.
13 M. Dirauf, D. Bandelli, C. Weber, H. Goerls, M. Gottschaldt and U. S. Schubert, *Macromol. Rapid Commun.*, 2018, **39**, 1800433.
14 C. Shi, Y. Guo, Y. Wu, Z. Li, Y. Wang, F. Du and Z. Li, *Macromolecules*, 2019, **52**, 4260–4269.
15 T. F. Burton, J. Pinaud and O. Giani, *Macromolecules*, 2020, **53**, 6598–6607.
16 M. Dirauf, A. Erlebach, C. Weber, S. Hoeppener, J. R. Buchheim, M. Sierka and U. S. Schubert, *Macromolecules*, 2020, **53**, 3580–3590.
17 J. Lian, M. Li, S. Wang, Y. Tao and X. Wang, *Macromolecules*, 2020, **53**, 10830–10836.
18 T. F. Burton, J. Pinaud, N. Petry, F. Lamaty and O. Giani, *ACS Macro Lett.*, 2021, **10**, 1454–1459.
19 B. Robertz, H. Keul and H. Hocker, *Macromol. Chem. Phys.*, 1999, **200**, 1034–1040.
20 T. Fey, H. Keul and H. Hocker, *Macromol. Chem. Phys.*, 2003, **204**, 591–599.
21 Y. Liang, J.-L. Pan, L.-H. Sun, J.-M. Ma, H. Jiang and Z.-L. Li, *Macromol. Rapid Commun.*, 2019, **40**, 1900435.
22 P. Ranganathan, C.-W. Chen, S.-P. Rwei, Y.-H. Lee and S. K. Ramaraj, *Polym. Degrad. Stab.*, 2020, **181**, 109323.
23 H. Gao, Y. Bai, H. Liu and J. He, *Ind. Eng. Chem. Res.*, 2019, **58**, 21872–21880.
24 A. Takahashi, *J. Macromol. Sci., Part A: Pure Appl.Chem.*, 1977, **11**, 411–420.
25 D. C. Christova, R. S. Velichkova and I. M. Panayotov, *Macromol. Chem. Phys.*, 1995, **196**, 3605–3613.
26 T. Xia, T.-J. Yue, G.-G. Gu, Z.-Q. Wan, Z.-L. Li and W.-M. Ren, *Eur. Polym. J.*, 2020, **136**, 109900.
27 J. Xu and N. Hadjichristidis, *Angew. Chem., Int. Ed.*, 2021, **60**, 6949–6954.
28 R. C. Pratt, B. G. G. Lohmeijer, D. A. Long, P. N. P. Lundberg, A. P. Dove, H. Li, C. G. Wade, R. M. Waymouth and J. L. Hedrick, *Macromolecules*, 2006, **39**, 7863–7871.
29 C. Aleman, O. Betran, J. Casanovas, K. N. Houk and H. K. Hall Jr., *J. Org. Chem.*, 2009, **74**, 6237–6244.
30 A. Duda, A. Kowalski, J. Libiszowski and S. Penczek, *Macromol. Symp.*, 2005, **224**, 71–83.
31 M. Hong and E. Y. X. Chen, *Nat. Chem.*, 2016, **8**, 42–49.
32 T. Fey, H. Keul and H. Hocker, *Macromolecules*, 2003, **36**, 3882–3889.
33 B. Robertz, H. Keul and H. Hocker, *Macromol. Chem. Phys.*, 1999, **200**, 1041–1046.

 This journal is © The Royal Society of Chemistry 2022

Published on 12 July 2022. Downloaded by Institute of Chemistry, CAS on 5/7/2026 9:22:57 AM.

34 B. Robertz, H. Keul and H. Hocker, *Macromol. Chem. Phys.*, 1999, **200**, 2100–2106.
35 H. Keul, B. Robertz and H. Hocker, *Macromol. Symp.*, 1999, **144**, 47–61.
36 H. Keul and H. Hocker, *Macromol. Rapid Commun.*, 2000, **21**, 869–883.
37 T. Fey, M. Holscher, H. Keul and H. Hocker, *Polym. Int.*, 2003, **52**, 1625–1632.
38 S. Gabriel, *Ber. Dtsch. Chem. Ges*, 1905, **38**, 2389–2404.
39 O. Nunez, J. Rodriguez and L. Angulo, *J. Phys. Org. Chem.*, 1994, **7**, 80–89.
40 P. Jangili and B. Das, *Synlett*, 2016, **27**, 924–928.
41 M. Tamura, R. Tamura, Y. Takeda, Y. Nakagawa and K. Tomishige, *Chem. Commun.*, 2014, **50**, 6656–6659.
42 K. K. Krawczyk, D. Madej, J. K. Maurin and Z. Czarnocki, *Tetrahedron: Asymmetry*, 2011, **22**, 1103–1107.
43 E. Koyama, F. Sanda and T. Endo, *Macromol. Symp.*, 1997, **122**, 275–280.
44 B. G. G. Lohmeijer, R. C. Pratt, F. Leibfarth, J. W. Logan, D. A. Long, A. P. Dove, F. Nederberg, J. Choi, C. Wade, R. M. Waymouth and J. L. Hedrick, *Macromolecules*, 2006, **39**, 8574–8583.
45 W. H. Stewart and T. H. Siddall, *Chem. Rev.*, 1970, **70**, 517–551.
46 W. J. Wedemeyer, E. Welker and H. A. Scheraga, *Biochemistry*, 2002, **41**, 14637–14644.
47 M. P. Hinderaker and R. T. Raines, *Protein Sci.*, 2003, **12**, 1188–1194.
48 J. A. Hodges and R. T. Raines, *Org. Lett.*, 2006, **8**, 4695–4697.
49 A. L. Bartuschat, K. Wicht and M. R. Heinrich, *Angew. Chem., Int. Ed.*, 2015, **54**, 10294–10298.
50 A. P. Dove, R. C. Pratt, B. G. G. Lohmeijer, R. M. Waymouth and J. L. Hedrick, *J. Am. Chem. Soc.*, 2005, **127**, 13798–13799.
51 Y. Yu, L.-M. Fang, Y. Liu and X.-B. Lu, *ACS Catal.*, 2021, **11**, 8349–8357.
52 J. Zhu and E. Y. X. Chen, *Angew. Chem., Int. Ed.*, 2018, **57**, 12558–12562.
53 Y. Xu, T. Şucu, M. R. Perrya and M. P. Shaver, *Polym. Chem.*, 2020, **11**, 4928–4932.
54 Y. Bernhard, L. Pagies, S. Pellegrini, T. Bousquet, A. Favrelle, L. Pelinski, P. Gerbaux and P. Zinck, *Green Chem.*, 2019, **21**, 123–128.
55 S. S. Rogers and L. Mandelkern, *J. Phys. Chem.*, 1957, **61**, 985–990.
56 R. C. Pratt, B. G. G. Lohmeijer, D. A. Long, R. M. Waymouth and J. L. Hedrick, *J. Am. Chem. Soc.*, 2006, **128**, 4556–4557.
57 G. L. Baker, E. B. Vogel and M. R. Smith III, *Polym. Rev.*, 2008, **48**, 64–84.
58 A. Sangroniz, J.-B. Zhu, X. Tang, A. Etxeberria, E. Y. X. Chen and H. Sardon, *Nat. Commun.*, 2019, **10**, 3559.
59 X. Liu, M. Hong, L. Falivene, L. Cavallo and E. Y. X. Chen, *Macromolecules*, 2019, **52**, 4570–4578.
60 C. Shi, L. T. Reilly, V. S. P. Kumar, M. W. Coile, S. R. Nicholson, L. J. Broadbelt, G. T. Beckham and E. Y. X. Chen, *Chem*, 2021, **7**, 2896–2912.
61 G. W. Coates and Y. D. Y. L. Getzler, *Nat. Rev. Mater.*, 2020, **5**, 501–516.
62 X. Tang and E. Y. X. Chen, *Chem*, 2019, **5**, 284–312.
63 X. B. Lu, Y. Liu and H. Zhou, *Chem. – Eur. J.*, 2018, **24**, 11255–11266.
64 M. Hong and E. Y. X. Chen, *Green Chem.*, 2017, **19**, 3692–3706.